Journal of Cerebral Blood Flow & Metabolism
23:285–300 © 2003 The International Society for Cerebral Blood Flow and Metabolism
Published by Lippincott Williams & Wilkins, Inc., Philadelphia

Imaging Human Mesolimbic Dopamine Transmission With Positron Emission Tomography. Part II: Amphetamine-Induced Dopamine Release in the Functional Subdivisions of the Striatum

*Diana Martinez, *Mark Slifstein, *Allegra Broft, *†Osama Mawlawi, *Dah-Ren Hwang, *†Yiyun Huang, *Thomas Cooper, *Lawrence Kegeles, *Eric Zarahn, *†Anissa Abi-Dargham, ‡§Suzanne N. Haber, and *†Marc Laruelle

*Departments of *Psychiatry and †Radiology, Columbia University College of Physicians and Surgeons, New York, New York, and Departments of ‡Neurobiology and §Anatomy, University of Rochester School of Medicine, Rochester, New York, U.S.A.*

Summary: The human striatum is functionally organized into limbic, associative, and sensorimotor subdivisions, which process information related to emotional, cognitive, and motor function. Dopamine projections ascending from the midbrain provide important modulatory input to these striatal subregions. The aim of this study was to compare activation of dopamine D_2 receptors after amphetamine administration in the functional subdivisions of the human striatum. D_2 receptor availability (V_3'') was measured with positron emission tomography and [^{11}C]raclopride in 14 healthy volunteers under control conditions and after the intravenous administration of amphetamine (0.3 mg/kg). For each condition, [^{11}C]raclopride was administered as a priming bolus followed by constant infusion, and measurements of D_2 receptor availability were obtained under sustained binding equilibrium conditions. Amphetamine induced a significantly larger reduction in D_2 receptor availability ($\Delta V_3''$) in limbic (ventral striatum, −15.3 ± 11.8%) and sensorimotor (postcommissural putamen, −16.1 ± 9.6%) regions compared with associative regions (caudate and precommissural putamen, −8.1 ± 7.2%). Results of this region-of-interest analysis were confirmed by a voxel-based analysis. Correction for the partial volume effect showed even greater differences in $\Delta V_3''$ between limbic (−17.8 ± 13.8%), sensorimotor (−16.6 ± 9.9%), and associative regions (−7.5 ± 7.5%). The increase in euphoria reported by subjects after amphetamine was associated with larger $\Delta V_3''$ in the limbic and sensorimotor regions, but not in the associative regions. These results show significant differences in the dopamine response to amphetamine between the functional subdivisions of the human striatum. The mechanisms potentially accounting for these regional differences in amphetamine-induced dopamine release within the striatum remain to be elucidated, but may be related to the asymmetrical feed-forward influences mediating the integration of limbic, cognitive, and sensorimotor striatal function via dopamine cell territories in the ventral midbrain. **Key Words:** Dopamine—D_2 receptor—[^{11}C]Raclopride—PET—Amphetamine—Psychostimulants.

Over the last decade, several groups have shown that imaging striatal dopamine D_2 receptors with positron emission tomography (PET) or single-photon emission computerized tomography (SPECT) in humans can be applied to measure acute changes in the concentration of synaptic dopamine (for review, see Laruelle, 2000). For example, the administration of psychostimulants such as amphetamine or methylphenidate is associated with an acute reduction in the binding potential (BP) of the radiotracers [^{11}C]raclopride or [^{123}I]IBZM (Volkow et al., 1994; Laruelle et al., 1995; Breier et al., 1997). In nonhuman primates, the magnitude of this reduction is related to the amphetamine-induced increase in extracellular dopamine measured with microdialysis (Breier et al., 1997; Laruelle et al., 1997). Therefore, the decrease in [^{11}C]raclopride BP can be used as a noninvasive measure of the change in dopamine induced by the challenge. Binding competition between the endogenous transmitter and the radioligand is believed to be the critical mechanism underlying this interaction, although

Received July 29, 2002; final version received October 24, 2002; accepted October 25, 2002.

Supported by the Public Health Service (NIMH RO1-MH54192, NIMH K02 MH01603–0, NIDA RO1-DA10219–01) and the Lieber Center for Schizophrenia Research.

Address correspondence and reprint requests to Diana Martinez, M.D., New York State Psychiatric Institute/Columbia University, 1051 Riverside Drive, Box #31, New York, NY 10032, U.S.A.; e-mail: dm437@columbia.edu

DOI: 10.1097/01.WCB.0000048520.34839.1A

other phenomena, such as receptor internalization or polymerization, have also been implicated (Laruelle, 2000; Logan et al., 2001).

This imaging paradigm has been applied to study striatal dopamine transmission in health and disease. In healthy subjects, two findings have emerged from studies relating dopamine transmission and the subjective effects of psychostimulants. Laruelle et al. (1995) reported that the increase in euphoria produced by acute amphetamine administration was related to the decrease in striatal [^{123}I]IBZM BP induced by the challenge, suggesting that stimulation of striatal D_2 receptors mediates the euphorigenic effects of amphetamine. This observation was confirmed by Volkow et al. (1999*b*), using methylphenidate. In addition, Volkow et al. (1999*a*) observed that low D_2 receptor availability at baseline (before the challenge) was predictive of the positive effects of methylphenidate. In pathologic conditions, this challenge has been used as a probe of presynaptic dopamine function. Psychostimulant-induced dopamine release has been reported to be increased in untreated patients with schizophrenia and Tourette syndrome (Laruelle et al., 1996; Breier et al., 1997; Singer et al., 2002), normal in patients with mood disorders (Anand et al., 2000; Parsey et al., 2001), and blunted in chronic cocaine abusers (Volkow et al., 1997).

A limitation of the aforementioned studies is that dopamine transmission was measured at the level of the striatum as a whole. The striatum, however, is a heterogeneous structure that includes several anatomic and functional subdivisions. Cortico-striatal-thalamo-cortical loops provide a general framework for defining the functional subdivisions of the striatum based on their connections. The general scheme of these loops involves projections from the cortex to the striatum, to the internal segment of the globus pallidum (GPi) or the substantia nigra (SN), to the thalamus and back to the cortex. These loops have been functionally classified into limbic loops (medial prefrontal, orbitofrontal, and anterior cingulate cortex—ventral striatum–ventral pallidum/SN–mediodorsal thalamic nuclei–cortex), associative loops (associative areas of the cortex including dorsolateral prefrontal cortex—precommissural putamen and most of the caudate–GPi/SN –ventral anterior thalamic nuclei–cortex) and sensorimotor loops (primary motor and premotor cortex, and supplementary motor area—postcommissural putamen–GPi/SN–ventral anterior thalamic nuclei–cortex) (for review see Joel and Weiner, 2000). This framework can be used to subdivide the striatum into the ventral or limbic striatum (VST), involved in drive and motivation, the central or associative striatum (AST), involved in cognition, and the sensorimotor striatum (SMST), involved in locomotion.

Recent advances in PET camera resolution allow the measurement of dopamine transmission parameters in the substructures of the striatum (Drevets et al., 2001; Mawlawi et al., 2001). This article is part of a series of studies aimed at evaluating the feasibility and validity of measuring parameters of dopamine transmission in striatal substructures using PET in humans. In a previous study, we established the reliability of measuring D_2 receptor availability in striatal subregions, using a bolus–plus–constant-infusion paradigm with [^{11}C]raclopride and the high resolution ECAT EXACT HR+ scanner (Siemens/CTI, Knoxville, TN, U.S.A.) (Mawlawi et al., 2001). In this study, we used the same imaging technique to evaluate amphetamine-induced changes in [^{11}C]raclopride binding to D_2 receptors in the functional subdivisions of the human striatum.

MATERIALS AND METHODS

General design

The study was approved by the Institutional Review Boards of the Columbia Presbyterian Medical Center and the New York State Psychiatric Institute. Sixteen healthy control subjects participated in this study. All subjects underwent magnetic resonance imaging (MRI) and two scans with [^{11}C]raclopride: a baseline scan and a scan after amphetamine administration (0.3 mg/kg intravenously). One subject was unable to complete the amphetamine scan owing to nausea, and another subject was unable to complete the MRI. Therefore, we report on 14 subjects (aged 33 ± 7 y; 9 men, 5 women). Subjects were scanned in succession, and all complete experiments were included in the final data set (28 PET scans). All but one pair of PET studies were performed on the same day, with a minimal interval of 2 h between injections of [^{11}C]raclopride. For technical reasons, one subject underwent the baseline and postamphetamine scans at an 18-d interval.

Subjects

Inclusion criteria were the absence of past or present neurologic, medical, or psychiatric illnesses (including alcohol and drug abuse) and pregnancy. Clinical status was assessed by history, review of systems, physical examination, routine blood tests, urine toxicology and ECG. Subjects provided written informed consent.

Radiochemistry

[^{11}C]Raclopride was prepared as previously described (Mawlawi et al., 2001). The precursor for the preparation of [^{11}C]raclopride, *O*-desmethyl raclopride hydrobromide, was generously provided by the Astra Zeneca Pharmaceutical Company (London, U.K.).

Positron emission tomography experiments

[^{11}C]Raclopride was administered as a priming bolus followed by constant infusion for 90 minutes, as previously described (Mawlawi et al., 2001). The bolus to infusion ratio was 105 minutes (i.e., 53% of the dose was given in the bolus). This ratio was selected based on the optimization procedure published by Watabe et al. (2000). [^{11}C]Raclopride was delivered in a 60-mL saline solution. A bolus dose of 30 mL was administered for a period of 3 minutes using an IMED pump (PC-1; Gemini, San Diego, CA, U.S.A.). After the bolus, the pump was reset to deliver 26 mL at 0.28 cc/min for the remaining 90 minutes.

Positron emission tomography imaging was performed with the ECAT EXACT HR+ (Siemens/CTI) operated in the three-dimensional (3D) mode. This camera acquires 63 slices covering an axial field of view of 15.5 cm (axial sampling of 2.46 mm). The 3D mode in plane and axial resolutions are 4.4 and 4.1 mm full-width half-maximum (FWHM) at the center of the field of view, respectively. A 10-minute transmission scan was obtained before radiotracer injection. Emission data were collected in the 3D mode for 90 minutes as 24 successive frames of increasing duration (3 × 20 seconds, 2 × 1 minute, 2 × 2 minutes, 1 × 3 minutes, 16 × 5 minutes).

Four venous samples (collected at 40, 50, 60, and 70 minutes) were obtained and analyzed for plasma [^{11}C]raclopride concentration as previously described (Mawlawi et al., 2001). Parent compound plasma concentrations in these four samples were averaged to obtain [^{11}C]raclopride concentration at steady state (C_{SS}, $\mu Ci\ mL^{-1}$). Clearance ($L \cdot h^{-1}$) was calculated as the rate of infusion/C_{SS} and plasma free fraction (f_1) was measured by ultrafiltration as previously described (Mawlawi et al., 2001).

After the baseline scan, subjects were allowed to rest outside of the camera. After repositioning the subject in the camera, amphetamine (0.3 mg/kg) was given intravenously for 30 seconds. The second [^{11}C]raclopride administration was initiated 2 minutes after the amphetamine injection, with experimental parameters identical to the baseline scan. Subjects were under constant cardiovascular monitoring after the amphetamine challenge.

A venous sample was obtained at 40 minutes to measure amphetamine plasma levels. Amphetamine was quantitated as its *N*-heptafluorobutyryl derivative via gas chromatography–mass spectrometry using a capillary column with the mass spectrometer, with simultaneous ion monitoring in the negative chemical ionization mode and reactant gas methane–ammonia (95:5), as previously described (Kegeles et al., 1999).

Subjective response

The subjective response to amphetamine was evaluated using a simplified version of the Amphetamine Interview Rating Scale (Laruelle et al., 1995). Four items (euphoria, energy, restlessness, and anxiety) were rated on a scale of 1 (not at all) to 10 (most ever) at baseline (10 minutes before amphetamine) and after the administration of amphetamine (at 0, 5, 10, 20, 30, and 40 minutes). The area under the curve (AUC) of the change from baseline (Δ_{AUC}) for each of these items was used as the outcome measure for comparison with PET data.

Magnetic resonance imaging acquisition

The MRI scans were acquired on a GE 1.5 T Signa Advantage system (GE Medical Systems, Waukesha, WI, U.S.A.). A sagittal scout was initially performed to identify the plane of the anterior commissure (AC) and posterior commissure (PC). A transaxial T_1-weighted sequence with 1.5-mm slice thickness was then acquired in the coronal plane orthogonal to the AC–PC plane over the whole brain. The following parameters were used: 3D spoiled-gradient recalled-acquisition in the steady-state; repetition time, 34 ms; echo time, 5 ms; flip angle, 45°; slice thickness, 1.5 mm and zero gap; 124 slices; field of vision, 22 × 16 cm; width, 256 × 192 matrix, reformatted to 256 × 256, yielding a voxel size of 1.5 mm × 0.9 mm × 0.9 mm.

Image coregistration

Images were reconstructed with attenuation correction using the transmission data and a Shepp 0.5 filter (cutoff 0.5 cycles/projection rays). Image processing was performed with MEDx (Sensor Systems, Sterling, VA, U.S.A.) as previously described (Mawlawi et al., 2001). Briefly, correction for PET frame misalignment due to head movement and PET to MRI registration were performed using the within- and between-modality automatic image registration algorithms (Woods et al., 1992, 1993). Because noise introduces errors in automatic image registration processing (Woods et al., 1992), PET frames were first denoised using a level 2, order 5 Battle-Lemarie wavelet (Mawlawi et al., 2001). The denoised PET frame acquired from 40 to 45 minutes was chosen as the reference frame and was registered to the MRI. The transformation matrix (TM1) was saved. In 5 of 28 studies, the *a priori* selected frame of reference (40–45 minutes) resulted in a less than optimal registration to the MRI. In these cases, the following frame (45–50 minutes) was used successfully as the frame of reference. The remaining denoised PET frames were then registered to the reference image and each transformation matrix was saved (TM2). TM1 and TM2 were then applied consecutively to each of the original (not denoised) PET frames, to generate the time–activity curves.

Regions of interest

The striatum was divided into five anatomic regions of interest (ROIs) and three functional subdivisions (see Table 1 and Fig. 1).

Regions of interest. The ROIs included the VST, the dorsal caudate rostral to the AC (precommissural dorsal caudate [pre-DCA]), the dorsal putamen rostral to the AC (precommissural dorsal putamen [pre-DPU]), the caudate caudal to the AC (postcommissural caudate [post-CA]), and the putamen caudal to the AC (postcommissural putamen [post-PU]). The VST includes the nucleus accumbens, the ventral caudate rostral to the AC, and the ventral putamen rostral to the AC. The ROIs were traced on coronal planes of each subject's MRI. The criteria used for dividing the precommissural striatum into three regions (VST, pre-DCA and pre-DPU) on the MRI are provided in our previous report (Mawlawi et al., 2001). The post-CA and post-PU included caudate and putamen from the plane of the AC to the plane including the most caudal part of these regions. The striatum as a whole was derived as a spatially weighted average of the five ROIs. Activity from the left and right

TABLE 1. *Functional and anatomic subdivisions*

Functional subdivisions	Anatomic subdivisions
Limbic striatum (LST)	Ventral striatum (VST)
Associative striatum (AST)	Precommissural dorsal putamen (pre-DPU)
	Precommissural dorsal caudate (pre-DCA)
	Postcommissural caudate (post-CA)
Sensorimotor striatum (SMST)	Postcommissural putamen (post-PU)

Precommissural and postcommissural refer to rostral and caudal to the anterior commissure. The ventral striatum contains the nucleus accumbens, precommissural ventral putamen, and precommissural ventral caudate.

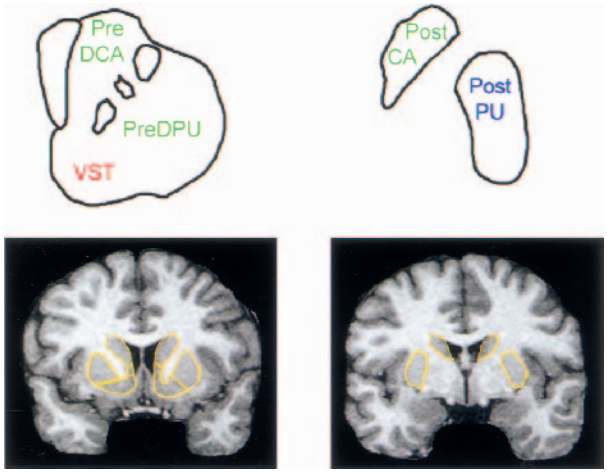

FIG. 1. Striatal subregions. **Top row:** schematic representation of striatal subregions. On the left, a coronal plane anterior to the plane of the anterior commissure (AC) is represented, including the VST (ventral striatum), the pre-DCA (precommissural dorsal caudate) and pre-DPU (precommissural dorsal putamen). On the right, a coronal plane posterior to the plane of the AC is presented, including the post-CA (postcommissural caudate) and post-PU (postcommissural putamen). Colors indicate functional subdivisions into limbic (red, VST), associative (green, pre-DCA, pre-DPU and post-CA) and sensorimotor (blue, post-PU) subdivisions. **Bottom row:** typical coronal magnetic resonance imaging scans at the level of the striatum, anterior (left) and posterior (right) to the plane of the AC, with boundaries of region of interest (yellow lines).

regions was averaged. The cerebellum (CER) was also drawn on the MRI and used as the reference region.

Functional subdivisions. Regions of interest were classified as belonging to the LST, AST, or SMST (Table 1). Measurements of the AST were derived as the spatially weighted average of the pre-DCA, pre-DPU, and post-CA. Although this classification best approximates the functional subdivisions of the striatum, some subtle anatomic points are neglected (for review, see Joel and Weiner, 2000). For example, most of the caudate is considered part of the associative circuit, although a relatively small dorsolateral portion belongs to SMST. Similarly, the most dorsolateral part of the putamen rostral to the AC belongs to SMST. Conversely, a small ventromedial part of the putamen caudal to the AC belongs to the associative and limbic circuits. In addition, at the most detailed anatomic level, a significant regional overlap exists between these circuits. Thus, the classification used here identifies these functional circuits only in a probabilistic sense: these regions correspond mostly, but not exclusively, to the various functional subdivisions of the striatum.

Derivation of outcome measures

D_2 receptor availability was estimated with the specific-to-nonspecific equilibrium partition coefficient (V_3''). Two analytical techniques were used to derive V_3'': an equilibrium analysis (Laruelle et al., 1994) and a simplified reference tissue kinetic model (SRTM) (Lammertsma and Hume, 1996). [^{11}C]Raclopride has a similar affinity for D_2 and D_3 receptors (Sokoloff et al., 1990), and, unless otherwise specified, we use the term D_2 receptors to denote both D_2 and D_3 receptors.

Equilibrium analysis was applied to the PET frames obtained from 40 to 90 minutes. The degree of equilibrium obtained during this time frame was assessed by measuring the change of the activity in the ROI over time. The slope of the ROI activity over time was expressed as a percentage of the mean value obtained from 40 to 90 minutes. The activity (μCi/mL) in the ROIs was averaged from 40 to 90 minutes. The nondisplaceable distribution volume (including free and nonspecifically bound radiotracer), V_2, was derived as the ratio of the activity in the cerebellum measured during the 40- to 90-minute period (A_{CER}) to C_{SS}. Specific binding was defined as the difference in activity in the ROI (A_{ROI}) and A_{CER}. V_3'' was then calculated as the ratio of specific to nonspecific binding (Laruelle et al., 1994):

$$V_3'' = (A_{ROI} - A_{CER})/A_{CER} \quad (1)$$

The SRTM analysis was implemented as previously described (Mawlawi et al., 2001) and applied to the entire data set (0–90 minutes).

In both analyses, the reduction in D_2 receptor availability after amphetamine ($\Delta V_3''$) was expressed in terms of the relative reduction in V_3'':

$$\Delta V_3'' = (V_3'' \text{ baseline} - V_3'' \text{ postamphetamine})/V_3'' \text{ baseline} \quad (2)$$

The relation between V_3'' and receptor parameters is described by $V_3'' = f_2 B_{max}/K_D$, where f_2 is the free fraction in nondisplaceable distribution volume, B_{max} is the number of available binding sites, and K_D is the [^{11}C]raclopride equilibrium dissociation constant. The relation between f_2 and f_1 is given by the inverse of the nondisplaceable distribution volume ($f_2 = f_1/V_2$).

Voxel-wise analysis

Voxel-based analysis was performed using Statistical Parametric Mapping 99 (SPM; Wellcome Department of Cognitive Neurology, University College London, U.K.). A mean PET image at equilibrium was created by averaging the MRI coregistered PET frames acquired during the equilibrium interval (40–90 minutes). Maps of V_3'' were created by applying Eq. 1 to all brain voxels of the mean PET images, using the value of A_{CER} derived from the ROI analysis. Maps of $\Delta V_3''$ were then created by applying Eq. 2 to the baseline and postamphetamine V_3'' maps. Each subject's MRI was normalized to the SPM T1-template image using SPM software, and the same transformation was applied to V_3'' PET maps. Smoothing with an isotropic Gaussian filter (FWHM = 4 mm), corresponding to twice the voxel size (normalized voxels are $2 \times 2 \times 2$ mm^3) was applied to conform to the SPM Gaussian field requirements. The significance of the amphetamine effect was assessed with a voxel-wise paired *t*-test, applied to the pre- and postamphetamine whole brain V_3'' maps. Cluster significance level was $P < 0.05$, after correction for multiple comparisons.

Partial volume effects correction

Partial volume effects (PVE) correction analysis was performed using a modification of the method of Rousset et al. (1998) as previously described (Mawlawi et al., 2001). Briefly, binary images were generated for each ROI from each subject's MRI, such that voxels contained within the ROI were set to 1 and all other voxels were set to 0 (n = 11 images per scan for the right and left VST, pre-DCA, pre-DPU, post-CA, post-PU and background). The binary images were then realigned to the location of the original PET images within the field of view, since the resolution of the PET camera varies within the field of view. These images were then smoothed using a model of the

point-spread function of the camera, creating 11 blurred image sets with voxel values between 1 and 0. The geometric transfer matrix (GTM), which describes the contribution of each source region to the measured regional activity, was generated. The true activity in each ROI was calculated by multiplying the vector of the regional measured activity by the inverse of the GTM. In this analysis, a "realistic" resolution model was applied, which takes into account the resolution of the PET camera, the reconstruction filter (Shepp 0.5), and subject movement during the scan (Mawlawi et al., 2001). This resolution model has a FWHM at the center of the field of view of 5.1 mm. Partial volume effects corrected V_3'' was calculated by applying Eq. 1 to PVE-corrected ROI activities, and PVE corrected $\Delta V_3''$ was calculated by applying Eq. 2 to PVE corrected V_3''.

Statistical analysis

Statistical analysis was performed with repeated measures ANOVA with condition (baseline and postamphetamine) as repeated factor (unless otherwise specified). *Post hoc* contrasts were assessed with Fisher's protected least significant difference. Relations between continuous variables were analyzed with the Pearson product moment correlation coefficient. A two-tailed probability value of $P < 0.05$ was selected as significant.

RESULTS

Scan parameters

Injected dose was 13.4 ± 3.8 mCi for the baseline scan and 10.9 ± 4.0 mCi for the postamphetamine scan (decay corrected for the time of infusion, $P = 0.01$). Specific activity at the start of infusion was 1,516 ± 751 Ci/mmol for the baseline scan and 1,608 ± 799 Ci/mmol for the postamphetamine scan ($P = 0.57$). The injected mass of raclopride was 3.4 ± 0.9 μg for the baseline scan and 2.8 ± 1.1 μg for the postamphetamine scan ($P = 0.10$).

Plasma analysis

The concentration of parent compound ([^{11}C]raclopride) was constant throughout the 40- to 90-minute period under both conditions, with an average change of −9 ± 23%/h for the baseline scan and 6 ± 27%/h after amphetamine ($P = 0.07$). None of these distributions were significantly different from zero (one-sample *t*-test). Total plasma activity increased over this time period, as expected owing to the increase in labeled metabolites of [^{11}C]raclopride (9 ± 18%/h at baseline, 15 ± 17%/h postamphetamine, $P = 0.12$). Conversely, the percent of the plasma activity that corresponded to the parent compound decreased over time (−13 ± 20%/h at baseline, −13 ± 16%/h postamphetamine, $P = 0.91$). Amphetamine had no effect on the clearance of the parent compound (baseline, 9.8 ± 2.7 L h^{-1}, postamphetamine, 9.5 ± 2.5 L h^{-1}, $P = 0.55$). No significant change in f_1 was observed between the baseline scan (3.7 ± 0.6%) and the postamphetamine scan (3.3 ± 0.5%, $P = 0.12$).

Cerebellum volume of distribution

The volume of distribution of the cerebellum (V_2) was 0.34 ± 0.08 mL g^{-1} at baseline and 0.34 ± 0.08 mL h^{-1} after amphetamine ($P = 0.59$). No correction was included for vascular volume in the calculation of V_2. The free fraction of the cerebellum (f_2) was 12 ± 5% for the baseline scan and 11 ± 4% for the postamphetamine scan ($P = 0.13$).

Region-of-interest volumes

The ROI volumes, as well as their contribution the total striatal volume, are listed in Table 2. The AST was the largest subdivision (contributing to 62 ± 3% of the whole striatum) followed by the SMST (27 ± 3%) and the LST (12 ± 4%).

Quality of equilibrium state

Activity in all ROIs decreased during the 40- to 90-minute interval as follows: −2.7 ± 11.6%/h (baseline) and −3.0 ± 12.5%/h (amphetamine condition) in the cerebellum; −4.9 ± 15.8%/h (baseline) and −8.4 ± 19.7%/h (amphetamine) in the VST; −11.9 ± 11.0%/h (baseline) and −11.4 ± 13.5%/h (amphetamine) for the pre-DCA; −7.2 ± 10.9%/h (baseline) and −9.7 ± 12.3%/h (amphetamine) in the pre-DPU; −11.8 ± 11.5%/h (baseline) and −13.4 ± 18.7%/h (amphetamine) for the post-CA; −11.0 ± 9.3%/h (baseline) and −10.4 ± 16.2%/h (amphetamine) in the post-PU. The decrease for each condition was significantly different from zero for all regions except for the cerebellum and VST (both baseline and amphetamine conditions). No significant differences in the slopes were observed between the baseline and amphetamine condition in any region.

Region-of-interest analysis

Figure 2 illustrates the time–activity curves of [^{11}C]raclopride during the bolus–plus–constant-infusion experiments obtained under control conditions and after injection of amphetamine in the same subject. Figure 3 shows the PET images of [^{11}C]raclopride distribution at baseline and after amphetamine in the same subject.

Equilibrium analysis. The values of V_3'' and $\Delta V_3''$ for each region are given in Table 3. Amphetamine produced a significant decrease in V_3'' in all regions ($P < 0.05$ for each region). The difference in $\Delta V_3''$ between regions was evaluated with repeated measures ANOVA, with

TABLE 2. *Regional volumes*

Subdivision	Region	Volume (mm^3)	Contribution to total striatal volume (%)
LST	VST	1,866 ± 641	12 ± 4
AST	—	9,669 ± 1,047	62 ± 3
—	Pre-DCA	4,677 ± 650	30 ± 3
—	Pre-DPU	3,355 ± 519	21 ± 2
—	Post-CA	1,637 ± 554	11 ± 4
SMST	Post-PU	4,144 ± 530	27 ± 3
STR	—	15,679 ± 1,501	100 ± 0

Values are mean ± SD; n = 14. LST, limbic striatum; VST, ventral striatum; AST, associative striatum; pre-DCA: precommissural dorsal caudate; pre-DPU, precommissural dorsal putamen; post-CA, postcommissural caudate; post-PU, post-commissural putamen; SMST, sensorimotor striatum; STR, striatum as a whole.

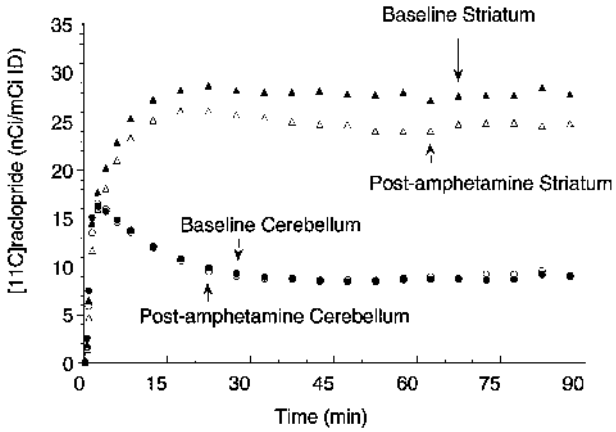

FIG. 2. Activity in the striatum (triangles) and cerebellum (circles) during bolus plus constant infusion of [^{11}C]raclopride at baseline (closed symbols) and after administration of amphetamine (0.3 mg/kg, open symbols). Amphetamine administration induced significant decrease in striatal activity but no change in cerebellum activity. Equilibrium measurements were obtained during the 40- to 90-minute interval.

regional $\Delta V_3''$ as repeated factor. Significant between-region differences in $\Delta V_3''$ were observed ($P = 0.002$). The regions fell into two groups: a high-displacement group that included the VST (−15.3 ± 11.8%) and post-PU (−16.1 ± 9.6%) and a low-displacement group that included the pre-DCA (−6.1 ± 7.6%), pre-DPU (−10.2 ± 7.9%), and post-CA (−7.6 ± 11.0%; Fig. 4). No significant differences in $\Delta V_3''$ were observed between the VST and post-PU, nor between the pre-DPU, pre-DCA, and post-CA. However, $\Delta V_3''$ in the VST was significantly higher than in the pre-DPU ($P = 0.04$), pre-DCA ($P = 0.0004$), and post-CA ($P = 0.003$). Similarly, $\Delta V_3''$ in post-PU was significantly higher than that in the pre-DPU ($P = 0.02$), pre-DCA ($P = 0.0001$), and post-CA ($P = 0.001$).

SRTM analysis. The values for V_3'' obtained using the SRTM analysis (Table 4) correlated very closely with the values obtained with the equilibrium analysis ($r > 0.9$, $P \leq 0.0001$ for all regions and all conditions). No significant differences were noted between V_3'' derived by equilibrium analysis and SRTM analysis (repeated measure ANOVA with analysis method as the repeated factor, $P > 0.05$ for all regions and conditions). The amphetamine-induced decrease in V_3'' using SRTM showed a pattern of displacement in the subregions similar to that seen with the equilibrium analysis. SRTM and equilibrium $\Delta V_3''$ were highly correlated ($r > 0.95$ in all regions) and not significantly different from each other ($P > 0.50$ for all regions).

Voxel-based analysis. Figure 5 shows the spatially normalized average $\Delta V_3''$ map. The majority of voxels with a displacement of 15% or greater are found in the VST and post-PU. This figure also illustrates the rostrocaudal gradient in $\Delta V_3''$ found in the putamen. The caudate is notably lacking in voxels with a large $\Delta V_3''$ value.

Figure 6 shows the *t* statistic for the amphetamine effect superimposed on the SPM canonical single-subject T1 image. The display threshold is $P \leq 0.001$, uncorrected. Significant clusters ($P < 0.05$, corrected) were detected in the VST and putamen, but not in the caudate (see Table 5). A small but significant cluster was also detected in the anterior cingulate, just below the genu of the corpus callosum (see transaxial image at the level of the AC–PC plane). In this analysis, with search volume corresponding to the entire brain, none of the peak voxels reached a corrected *P* value lower than 0.05. When the analysis was restricted to the striatum, peak voxels in clusters 1 and 2 had *P* corrected < 0.05, whereas the corrected *P* value for the peak voxel of cluster 3 was 0.052.

Partial volume effects correction

Values of V_3'' and $\Delta V_3''$ after PVE correction are listed in Table 6. Partial volume effects correction resulted in a significant increase in the measured values of V_3'' for

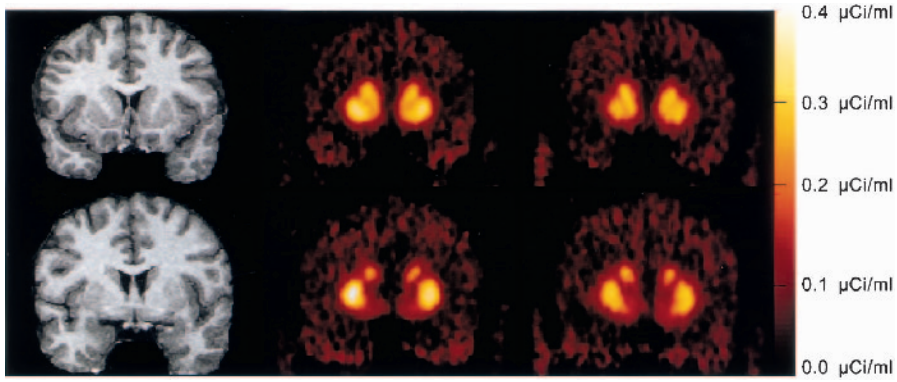

FIG. 3. Coregistered magnetic resonance imaging scans and positron emission tomography (PET) [^{11}C]raclopride coronal images (**upper row:** plane 6 mm anterior to the anterior commissure; **lower row:** plane of anterior commissure) during control (middle column) and postamphetamine (right column) experiments in the same subject. PET images represent a 10-minute acquisition obtained under equilibrium conditions, 40 to 50 minutes after initiation of [^{11}C]raclopride administration (bolus plus constant infusion). Color scale was coded as µCi/mL per mCi injected dose, to insure the comparability of the images. Amphetamine did not affect the background activity but reduced the activity in VST, pre-DPU and the post-PU. Changes in pre-DCA and caudate are less pronounced.

TABLE 3. *Effect of amphetamine on [^{11}C]raclopride V_3'': equilibrium analysis*

Subdivision	Region	Baseline V_3''	Postamphetamine V_3''	Difference (%)	*P* values
LST	VST	2.03 ± 0.34	1.71 ± 0.31	−15.3 ± 11.8	<0.001
AST	—	2.56 ± 0.31	2.34 ± 0.23	−8.1 ± 7.2	<0.001
—	Pre-DCA	2.44 ± 0.31	2.28 ± 0.25	−6.1 ± 7.6	<0.01
—	Pre-DPU	3.11 ± 0.35	2.78 ± 0.29	−10.2 ± 7.9	<0.001
—	Post-CA	1.77 ± 0.33	1.63 ± 0.30	−7.6 ± 11.0	<0.05
SMST	Post-PU	3.14 ± 0.39	2.62 ± 0.34	−16.1 ± 9.6	<0.001
STR	—	2.53 ± 0.24	2.26 ± 0.24	−10.3 ± 7.2	<0.001

Values are mean ± SD; n = 14.

AST values are calculated as the spatially weighted average of pre-DCA, pre-DPU, and post-CA. STR values are calculated as the spatially weighted average of the five regions of interest (VST, pre-DCA, pre-DPU, post-CA, post-PU).

LST, limbic striatum; VST, ventral striatum; AST, associative striatum; pre-DCA, precommissural dorsal caudate; pre-DPU, precommissural dorsal putamen; post-CA, postcommissural caudate; post-PU, postcommissural putamen; SMST, sensorimotor striatum; STR, striatum as a whole.

each ROI ($P < 0.05$ for all regions). This increase was the most pronounced in the post-CA, where PVE correction almost doubled V_3'' (93 ± 16%). The lowest increase was in the pre-DPU (47 ± 5%).

Partial volume effects correction resulted in small but significant changes in $\Delta V_3''$ in the striatal subregions. Partial volume effects correction increased $\Delta V_3''$ in regions with high $\Delta V_3''$ values (VST and post-PU). In the VST, $\Delta V_3''$ increased from −15.3 ± 11.8% to −17.8 ± 13.8% ($P < 0.01$). $\Delta V_3''$ also increased, to a lesser degree, in the post-PU (from −16.1 ± 9.6% to −16.6 ± 9.9%, $P < 0.01$). Conversely, PVE correction decreased $\Delta V_3''$ in regions with low values for $\Delta V_3''$. In the pre-DCA, $\Delta V_3''$ decreased from −6.1 ± 7.6 to −5.5 ± 7.9% ($P = 0.045$). In the pre-DPU, $\Delta V_3''$ decreased from −10.2 ± 7.9% to −9.4 ± 8.2% ($P = 0.02$). Partial volume effects correction had no significant effect on $\Delta V_3''$ in the post-CA (from −7.6 ± 11.0 to −7.8 ± 12.6%, $P = 0.78$). Partial volume effects did not affect the measurement of $\Delta V_3''$ at the level of the whole striatum ($P = 0.8$).

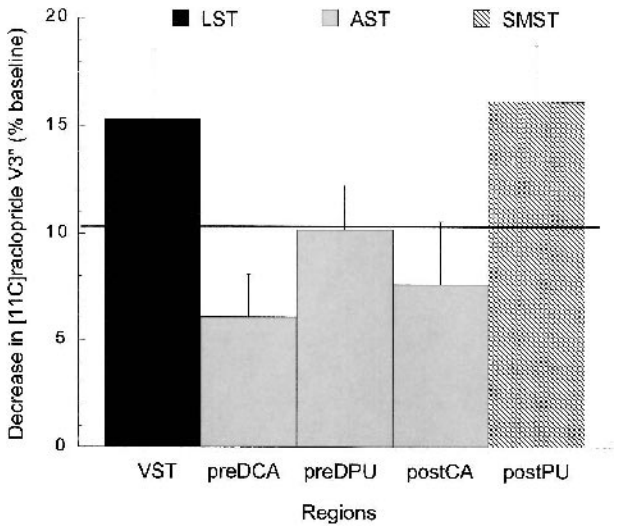

FIG. 4. Mean ± SEM decrease in [^{11}C]raclopride D_2 receptor availability (V_3'') expressed in percentage change from baseline ($\Delta V_3''$) in five subregions of the striatum in 14 healthy subjects after administration of 0.3 mg/kg amphetamine (equilibrium analysis, uncorrected for partial volume effects). Regions include: VST (ventral striatum), pre-DCA (precommissural dorsal caudate), pre-DPU (precommissural dorsal putamen), post-CA (postcommissural caudate) and post-PU (postcommissural putamen). Bar patterns represent the functional classification of these regions into limbic (black bar), associative (gray bars), and sensorimotor (striped bar) striata. The solid line represents the percent decrease seen in the striatum as a whole. Amphetamine induced significant reduction in [^{11}C]raclopride V_3'' in all regions. Significant between-region differences in the amphetamine effect were observed ($P = 0.002$), such that the LST and SMST $\Delta V_3''$ were significantly higher than $\Delta V_3''$ in post-CA, post-PU and pre-DPU ($P < 0.05$ for all contrasts). LST, limbic striatum; AST, associative (central) striatum; SMST, sensorimotor striatum.

The between-region differences in $\Delta V_3''$ after PVE correction were similar to the between-region differences seen in $\Delta V_3''$ before correction: the VST and pre-DPU were significantly higher than the three other regions (post-CA, post-PU and pre-DCA).

Plasma amphetamine levels

The mean plasma amphetamine level was 40.2 ± 13.6 ng/mL. No significant relationships were observed between amphetamine plasma levels and $\Delta V_3''$ in any of the ROIs (VST: $r = -0.16$, $P = 0.60$; pre-DCA: $r = -0.27$, $P = 0.36$; pre-DPU: $r = -0.16$, $P = 0.60$; post-CA: $r = -0.17$, $P = 0.56$; post-PU: $r = -0.31$, $P = 0.30$).

Subjective response

After amphetamine, subjects' ratings of euphoria and energy significantly increased (repeated measures ANOVA with time as repeated factor, $P < 0.0001$ and $P = 0.012$, respectively). Anxiety significantly decreased ($P = 0.012$). No significant changes were observed in restlessness ($P = 0.30$). No significant correlation was found between amphetamine plasma levels and changes in euphoria ($r = 0.34$, $P = 0.26$) and energy ($r = 0.41$, $P = 0.15$). Amphetamine plasma levels were associated with significant decrease in anxiety ($r = -0.69$, $P = 0.01$).

Of the four self-report items, only euphoria was significantly correlated with $\Delta V_3''$, such that a greater

TABLE 4. *Effect of amphetamine on [^{11}C]raclopride V_3'': simplified reference tissue model analysis*

Subdivision	Region	Baseline V_3''	Postamphetamine V_3''	Difference (%)	*P* values
LST	VST	2.04 ± 0.29	1.71 ± 0.29	−16.0 ± 11.6	<0.001
AST	—	2.52 ± 0.30	2.31 ± 0.23	−8.0 ± 6.6	<0.001
—	Pre-DCA	2.40 ± 0.30	2.25 ± 0.26	−6.0 ± 6.9	<0.01
—	Pre-DPU	3.07 ± 0.34	2.74 ± 0.31	−10.3 ± 7.5	<0.001
—	Post-CA	1.74 ± 0.31	1.61 ± 0.28	−7.0 ± 9.8	<0.05
SMST	Post-PU	3.08 ± 0.36	2.59 ± 0.33	−15.7 ± 9.0	<0.001
STR	—	2.61 ± 0.29	2.31 ± 0.25	−11.1 ± 7.0	<0.001

Values are mean ± SD; n = 14.

AST values are calculated as the spatially weighted average of pre-DCA, pre-DPU, and post-CA. STR values are calculated as the spatially weighted average of the five regions of interest (VST, pre-DCA, pre-DPU, post-CA, post-PU).

LST, limbic striatum; VST, ventral striatum; AST, associative striatum; pre-DCA, precommissural dorsal caudate; pre-DPU, precommissural dorsal putamen; post-CA, postcommissural caudate; post-PU, postcommissural putamen; SMST, sensorimotor striatum; STR, striatum as a whole.

increase in euphoria was associated with higher [^{11}C]raclopride displacement. This association was observed in the VST and SMST (Fig. 7), as well as at the level of the striatum as a whole ($r = 0.76$, $P = 0.002$). No significant association was seen between euphoria and any region of the AST as well as the AST itself. The other self-report items were not associated with $\Delta V_3''$ in any of the striatal subregions (data not shown).

No association was found between baseline V_3'' and amphetamine-induced changes in euphoria in any subregion (VST: $r = 0.05$, $P = 0.88$; post-CA: $r = 0.06$, $P = 0.83$; pre-DPU: $r = -0.03$, $P = 0.92$; post-CA: $r = 0.27$, $P = 0.35$; post-PU: $r = 0.18$, $P = 0.53$) or in the striatum as a whole ($r = 0.07$, $P = 0.81$).

DISCUSSION

The aim of this study was to evaluate amphetamine-induced changes in [^{11}C]raclopride V_3'' in the functional subdivisions of the human striatum. Significant differences were observed: the amphetamine effect was higher

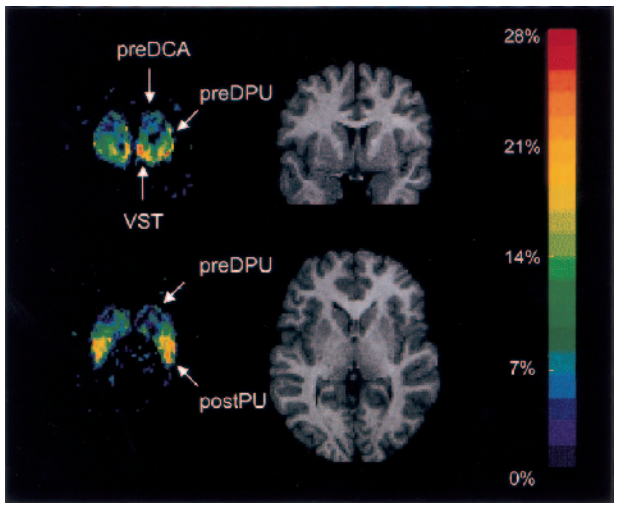

FIG. 5. Coronal and transaxial views of the $\Delta V_3''$ map normalized to the Montreal Neurological Institute T1-template magnetic resonance imaging (MRI) scan. The images represent the voxel-based average $\Delta V_3''$ across subjects. The color scale was coded to represent the percent decrease in V_3'' after amphetamine, from dark blue (0%) to red (–28%). For visual clarity, only voxels in which baseline V_3'' exceeded 1 are shown. The equivalent planes from one subject's normalized MRI scan are shown for comparison. These views illustrate the two locations of highest amphetamine effect. The coronal plane, at the level of the anterior striatum, shows high displacement in the VST, low displacement in the pre-DCA, and intermediate values in the pre-DPU. The transaxial view illustrates the second area of high displacement in the post-PU, and the rostrocaudal gradient of displacement in the putamen. Pre-DCA, precommissural dorsal caudate; pre-DPU, precommisural dorsal putamen; VST, ventral striatum; post-CA, postcommissural caudate; post-PU, postcommissural putamen.

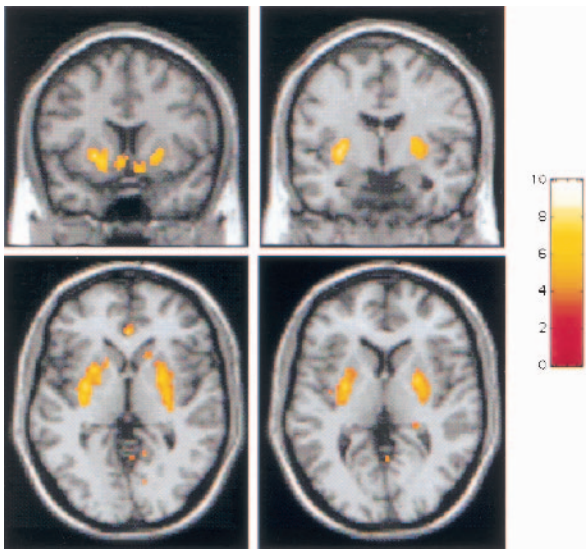

FIG. 6. Map of *t* values showing the voxels with significant decrease in V_3'' after amphetamine ($P \leq 0.001$, uncorrected). **Upper row**—left: coronal view, 10 mm rostral to the plane of the anterior commissure, showing significant clusters ($P < 0.001$, corrected) in the ventral striatum and precommissural dorsal putamen; right: coronal view, 4 mm caudal to the plane of the AC, showing significant clusters ($P < 0.001$, corrected) in the postcommissural putamen (post-PU). **Lower row**—left: transaxial view, at the level to the AC–PC plane, showing significant clusters in the post-PU, as well as a significant cluster in the anterior cingulate, just below the genu of the corpus callosum; right: transaxial view, 4 mm dorsal to the AC–PC plane, showing significant clusters in the post-PU. The absence of significant clusters in the caudate is noticeable. AC, anterior commissure; PC, posterior commissure.

TABLE 5. *Effect of amphetamine on [^{11}C]raclopride V_3'': statistical parametric mapping analysis*

	Cluster level			Voxel level				MNI			Tailarach		
Region	*P* corrected	K_E	*P* uncorrected	*P* corrected	T	Z	*P* uncorrected	x	y	z	x	y	z
L DPU	<0.001	620	<0.001	0.355	10	5.22	<0.001	−22	10	−2	−22	10	−2
	—	—	—	0.604	9.16	5.03	<0.001	−30	−2	−2	−30	−2	−2
	—	—	—	0.997	7.31	4.53	<0.001	−32	−12	0	−32	−12	1
R DPU	<0.001	414	<0.001	0.737	8.77	4.93	<0.001	26	2	2	26	2	2
	—	—	—	1	6.79	4.36	<0.001	30	−12	0	30	−12	1
	—	—	—	1	6.74	4.35	<0.001	22	10	−4	22	10	−4
R VST	<0.001	62	<0.001	1	5.94	4.06	<0.001	10	12	−12	10	11	−11
R CIN	0.046	31	<0.001	0.719	8.82	4.95	<0.001	2	36	0	2	35	−2

MNI column contains spatial coordinates in MNI canonical magnetic resonance imaging; Tailarach, spatial coordinates in the Tailarach atlas.

K_E, number of voxels in the cluster; MNI, Montreal Neurological Institute; DPU, dorsal putamen; VST, ventral striatum; CIN, anterior cingulate; L, R, left and right.

in the limbic and sensorimotor subdivisions compared with the associative subdivision. These regional differences do not seem to be due to artifacts of the imaging process: the paired-bolus–plus–infusion protocol provided an unbiased estimate of V_3'', both ROI and voxel-wise analyses showed the same pattern of effect, and the findings were confirmed after PVE correction.

Paired-bolus–plus–infusion protocol

The accurate measurement of changes in D_2 receptor availability after a psychostimulant challenge requires a quantitative approach that is not affected by changes in regional CBF or peripheral clearance of the radiotracer induced by the challenge (see discussion in Laruelle, 2000). In this study, we used a new approach to this measurement (paired-bolus–plus–constant-infusion studies), which provides several advantages over previously used methods.

The most frequently used method to evaluate changes in [^{11}C]raclopride V_3'' after a challenge is to perform two experiments with a single-bolus [^{11}C]raclopride injection (Volkow et al., 1994, 1997, 1999*b*; Drevets et al., 2001). This method, however, is associated with several inconveniences: (1) If regional CBF significantly varies during the time frame of the scan, the measurement of V_3'' may be affected; (2) although V_3'' can be derived without an arterial input function, an arterial line is needed to derive distribution volumes, which is desirable for between-subject comparisons; (3) PVE correction on kinetic data requires correction on each individual frame, since the relative concentrations of activity in the ROIs change over time.

A second method to evaluate $\Delta V_3''$ after a challenge is to administer the tracer as a bolus followed by a constant infusion and to obtain the baseline and postchallenge measurements over the course of a single study. This method has been used extensively with [^{123}I]IBZM (Laruelle et al., 1995; Abi-Dargham et al., 1998; Kegeles et al., 1999; Anand et al., 2000; Parsey et al., 2001) and [^{11}C]raclopride (Breier et al., 1997; Watabe et al., 2000). The bolus–plus–constant-infusion technique circumvents some of the difficulties associated with the paired single-bolus paradigm (Carson et al., 1993; Laruelle et al., 1995; Mawlawi et al., 2001) as follows: (1) Under sustained equilibrium conditions, there is no net transfer of the radiotracer in and out of the brain, and the uptake is insensitive to changes in regional CBF; (2) The bolus–plus–constant-infusion paradigm allows measurement of

TABLE 6. *Effect of amphetamine on [^{11}C]raclopride V_3'': equilibrium analysis after partial volume effect correction*

Subdivision	Region	Baseline V_3''	Postamphetamine V_3''	Difference (%)	*P* values
LST	VST	3.51 ± 0.84	2.87 ± 0.69	−17.8 ± 13.8	<0.001
AST	—	3.96 ± 0.46	3.64 ± 0.35	−7.5 ± 7.5	<0.001
—	Pre-DCA	3.75 ± 0.48	3.53 ± 0.39	−5.5 ± 7.9	<0.01
—	Pre-DPU	4.57 ± 0.53	4.12 ± 0.46	−9.4 ± 8.2	<0.001
—	Post-CA	3.45 ± 0.79	3.16 ± 0.75	−7.8 ± 12.6	<0.05
SMST	Post-PU	5.48 ± 0.85	4.54 ± 0.71	−16.6 ± 9.9	<0.001
STR	—	4.01 ± 0.55	3.58 ± 0.45	−10.5 ± 7.5	<0.001

Values are mean ± SD; n = 14.

AST values are calculated as the spatially weighted average of pre-DCA, pre-DPU, and post-CA. STR values are calculated as the spatially weighted average of the five regions of interest (VST, pre-DCA, pre-DPU, post-CA, post-PU).

LST, limbic striatum; VST, ventral striatum; AST, associative striatum; pre-DCA, precommissural dorsal caudate; pre-DPU, precommissural dorsal putamen; post-CA, postcommissural caudate; post-PU, postcommissural putamen; SMST, sensorimotor striatum; STR, striatum as a whole.

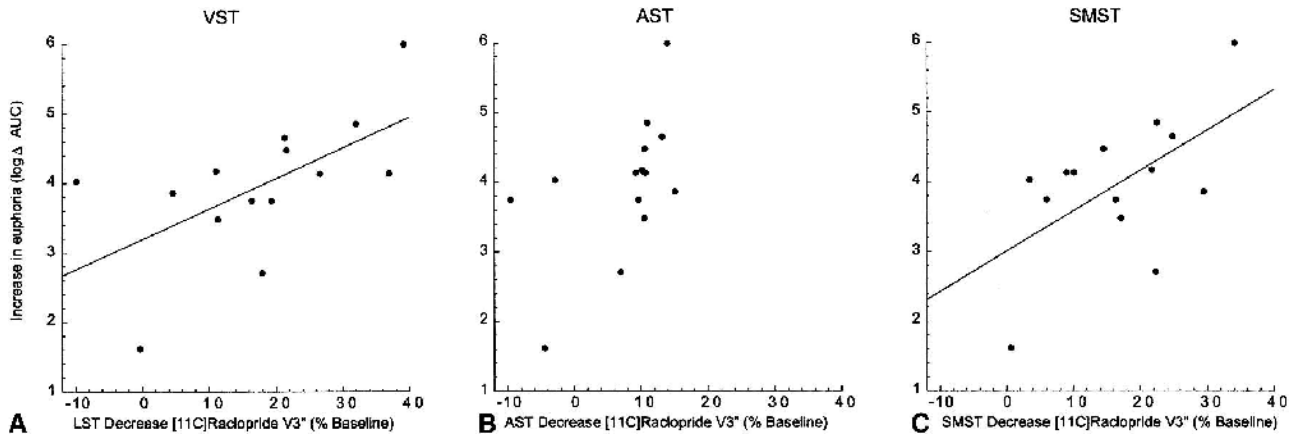

FIG. 7. Correlation between subjective report of amphetamine-induced euphoria and decrease in [^{11}C]raclopride V_3'' in the limbic striatum (LST; **A**), associative (central) striatum (AST; **B**), and sensorimotor striatum (SMST; **C**). A significant correlation was found between change in euphoria (calculated as the area under the curve, Δ_{AUC}) and $\Delta V_3''$ in the LST ($r2 = 0.33$, $P = 0.03$) and SMST ($r2 = 0.34$, $P = 0.03$) but not in the AST ($r2 = 0.15$, $P = 0.42$). The partial volume effects corrected data were used in this figure. Similar results were seen with the non–partial volume effects corrected values. For clarity of display, the x-axes were kept constant for the three regions, and the y-axes show log Δ_{AUC}.

distribution volumes without arterial sampling because arterial and venous concentrations of the radiotracer equilibrate; (3) The bolus–plus–constant-infusion method allows more efficient PVE correction because it is applied only once, using the mean measured ROI activity acquired during the equilibrium interval.

Despite these advantages, initial experiments in our laboratory showed that the single-bolus–plus–constant-infusion protocol was problematic for measuring amphetamine-induced changes in [^{11}C]raclopride V_3'' in the subregions of the striatum. It takes about 40 minutes of infusion for [^{11}C]raclopride to reach equilibrium (Breier et al., 1997; Watabe et al., 2000; Mawlawi et al., 2001). Assuming the prechallenge measurement is obtained during 10 minutes (40- to 50-minute interval), the earliest time point at which amphetamine can be given is at 50 minutes. It then takes another 20 to 30 minutes for [^{11}C]raclopride to dissociate and reach a new equilibrium, such that the postamphetamine measurement cannot begin until 70 to 80 minutes into the scan. Therefore, the postchallenge measurement must be performed after considerable decay of the isotope. This factor was a concern for the measurement of the striatal subregions, since high counting statistics are needed to preserve resolution.

Therefore, we modified this protocol such that two studies were performed with a bolus plus constant infusion of [^{11}C]raclopride, one at baseline and the second after amphetamine. Like the paired single-bolus protocol, the paired-bolus–plus–constant-infusion protocol provides better and equal counting statistics for the measurement of both pre- and postamphetamine V_3'', while maintaining the advantages of this method. This approach takes advantage of the long-lasting effect of amphetamine on D_2 receptor availability. Recent experiments performed with [^{11}C]raclopride (Carson et al., 2001) have confirmed the initial observation made with [^{123}I]IBZM that the effect of amphetamine on D_2 receptor BP is stable and prolonged (>4 h) (Laruelle et al., 1997). Because the applicability of this methodology rests on the long duration of the amphetamine effect, it should not be used for other challenges without appropriate validation.

A limitation of the bolus-plus-infusion protocol is that an appropriate equilibrium state may not be established in every subject during the *a priori* selected scanning period. The degree of equilibrium was assessed by measuring the change in ROI activity during the 40- to 90-minute period. In the present study, we replicated our previous observation that this protocol (K_{bol} of 105 minutes) is associated with a decrease in [^{11}C]raclopride activity of about 10%/h during the 40- to 90-minute interval (Mawlawi et al., 2001). This observation suggests that equilibrium is not completely achieved at 40 minutes and that K_{bol} should be slightly reduced. However, V_3'' values derived with the equilibrium analysis of the 40- to 90-minute interval were not significantly different from V_3'' values derived using SRTM and the full data set. Because the SRTM does not require sustained equilibrium, this result indicates that this issue has a negligible impact on the derivation of V_3'' using the equilibrium approach.

Finally, the use of V_3'' as an outcome measure to estimate the effect of amphetamine on D_2 receptor availability implies that f_2 is unaffected by amphetamine. This assumption was validated in this data set, supporting the use of $\Delta V_3''$ to estimate the reduction in B_{max}/K_D ratio induced by the challenge. Together, these considerations support the robustness of the imaging method used in this study for the quantification of the change in D_2 receptor availability after a challenge.

Region-of-interest analysis

The decrease in [^{11}C]raclopride V_3'' measured at the level of the whole striatum in this study was −10.3 ± 7.2% (n = 14). Using [^{123}I]IBZM, we previously observed a striatal $\Delta V_3''$ of −8.7 ± 7.2% after the same dose of amphetamine in healthy volunteers (n = 43, aged 38 ± 10 y, 36 men and 7 women). This $\Delta V_3''$ value was derived from pooling four independent samples studied under identical experimental conditions (Laruelle et al., 1995, 1996; Abi-Dargham et al., 1998; Kegeles et al., 1999) and was not statistically different from $\Delta V_3''$ measured with [^{11}C]raclopride in the present study (P = 0.21, unpaired t-test).

The specific aim of this study was to examine the impact of amphetamine on dopamine transmission in the limbic, associative, and sensorimotor subdivisions of the striatum. Analysis of the PET data showed that amphetamine induced a significantly larger reduction in D_2 receptor availability in the limbic (−15.3 ± 11.8%) and sensorimotor (−16.1 ± 9.6%) regions compared with the associative regions (−8.1 ± 7.2%) of the striatum.

In a previous study of 7 healthy volunteers, Drevets et al. (2001) also studied the effect of amphetamine in striatal subregions. That study was performed with the same radiotracer, the same dose of intravenous amphetamine, and the same camera as the present study, although a different protocol (paired single-bolus studies), a different analytical approach (SRTM), and different striatal subregions were used. Although the criteria used to delineate the VST and pre-DCA differed between the two studies, both sets of criteria are expected to identify similar regions. Ventral striatum $\Delta V_3''$ measured in this study (−15.3 ± 11.8%) was in close agreement with VST $\Delta V_3''$ reported by Drevets et al. (2001) (−15.4 ± 10.6%). The pre-DCA $\Delta V_3''$ measured here (−6.1 ± 7.6%) was also consistent with that reported in the dorsal caudate (−4.5 ± 8.2%) by Drevets et al. (2001).

Comparison of results within the putamen are more difficult because the main difference between the subregions in the present study and those of Drevets et al. (2001) is the method used to subdivide the putamen. In the present study, the plane of the AC was used to divide the putamen into its associative (precommissural) and sensorimotor (postcommissural) compartments along its rostrocaudal axis. A significant difference was found between these compartments: pre-DPU $\Delta V_3''$ (−10.2 ± 7.9%) was significantly lower than post-PU $\Delta V_3''$ (−16.1 ± 9.6%, $P < 0.04$). In contrast, Drevets et al. (2001) subdivided the putamen into two parts along its dorsoventral axis, and reported $\Delta V_3''$ of −10.2 ± 10.6% in the dorsal putamen and −14.9 ± 10.1% in the ventral putamen.

To improve the comparability between the studies, we reanalyzed our data using the regional criteria provided for the dorsal and ventral putamen in the study by Drevets et al. (2001). Using these criteria, we measured a $\Delta V_3''$ of −11.5 ± 10.3% and −15.2 ± 9.8% in the dorsal and ventral putamen, respectively, which are consistent with the decreases reported by Drevets et al. (2001). The difference between dorsal and ventral putamen $\Delta V_3''$ was not significant (P = 0.23), suggesting that $\Delta V_3''$ varies within the putamen along a rostrocaudal rather than a dorsoventral gradient. Nevertheless, the high degree of correlation between the results of both studies is perhaps the best demonstration of the suitability of current PET technology to measure these subtle effects in these small and adjacent regions.

Voxel-based analysis

Voxel-based analysis has some advantages over ROI analysis: it is less labor intensive and allows the detection of effects whose location are not within anatomically predefined regions. Voxel-based methods, however, involve spatial normalization and smoothing, which may limit the power to detect changes in small and anatomically predefined regions. Therefore, in this study we performed both ROI and voxel-based analyses, to compare the results generated by both techniques.

Using voxel-based analysis, significant $\Delta V_3''$ clusters were seen in the VST and putamen, and no significant clusters were detected in the caudate. This result was generally consistent with the results of the ROI analysis, except that $\Delta V_3''$ in the caudate was significant in the ROI analysis. The discrepancy between the ROI-based and voxel-based analyses of the caudate suggest a loss of power associated with the voxel-based method and prompted us to examine in more detail the factors that may account for this difference. Since the SPM analysis included the whole brain as the search volume, the absence of significant clusters in the caudate was thought to be related to the penalty imposed by the large search volume. However, even after restricting the search volume to the caudate alone no significant clusters were detected in this region (data not shown).

Since the voxel-based analysis involves both spatial smoothing and normalization of the data, we investigated this issue further by performing an ROI analysis on V_3'' maps that had been either smoothed, normalized, or both. Four analyses were generated: (1) individual ROIs were applied to the individual original V_3'' maps (without smoothing or normalization); 2) individual ROIs were applied to individual V_3'' maps smoothed using a 4-mm FWHM filter (no normalization); (3) a set of ROIs drawn on the Montreal Neurological Institute single-subject T1 template was applied to spatially normalized (but not smoothed) V_3'' maps; and (4) this set of template ROIs was applied to spatially normalized and smoothed V_3'' maps.

The results from this comparison (Table 7) showed that smoothing and normalization, alone or in combination,

TABLE 7. *Impact of spatial smoothing and normalization on $\Delta V_3''$*

Region	No smoothing or normalization	Smoothed only	Normalized only	Smoothed and normalized
VST	−14.4 ± 10.6% (<0.001)	−14.0 ± 10.7% (<0.001)	−11.8 ± 9.9% (<0.001)	−11.7 ± 9.5% (<0.001)
Pre-DCA	−5.9 ± 7.6% (<0.01)	−5.8 ± 7.6% (<0.01)	−5.9 ± 7.5% (<0.01)	−5.9 ± 7.6% (<0.01)
Pre-DPU	−10.1 ± 7.8% (<0.001)	−10.1 ± 7.8% (<0.001)	−8.4 ± 7.4% (<0.001)	−9.0 ± 6.6% (<0.001)
Post-CA	−6.9 ± 12.7% (0.05)	−6.6 ± 12.1% (<0.05)	−7.2 ± 12.3% (<0.05)	−7.2 ± 11.8% (<0.05)
Post-PU	−15.8 ± 10.2% (<0.001)	−15.4 ± 9.9% (<0.001)	−15.4 ± 8.3% (<0.0001)	−15.1 ± 8.2% (<0.0001)

Values are mean ± SD $\Delta V_3''$ in four sets of region-of-interest analyses of V_3'' maps (see Discussion for details). Values in parentheses are *P* values of the amphetamine effect (repeated measure ANOVA, with condition as repeated factor). No significant differences were observed in $\Delta V_3''$ between methods (repeated measure ANOVA with method as repeated factor, $P > 0.05$ for all regions).

VST, ventral striatum; pre-DCA, precommissural dorsal caudate; pre-DPU, precommissural dorsal putamen post-CA, postcommissural caudate; post-PU, postcommissural putamen.

had virtually no effect on $\Delta V_3''$ itself or its significance level. Evidently, the loss of power observed in the SPM analysis was not due to spatial normalization or smoothing, but rather to the intrinsic voxel-by-voxel analytic process and its correction for multiple comparisons.

From this set of analyses, we conclude that, when a hypothesis pertains to an *a priori* defined ROI, it is best tested at the ROI level rather than in SPM. However, at least in healthy subjects, the spatial normalization preserves the anatomic integrity of the striatal subregions, and the information derived from a generic ROI on spatially normalized data is comparable to the information derived from the much more labor-intensive individual ROI analysis.

Partial volume effects correction

The limited resolution of the imaging process results in signal blurring (activity spilling over across regions). The quantification of activity in a given ROI is therefore affected by two reciprocal interactions. First, a proportion of the activity originating in the ROI will be recorded outside of this region (spill-out), resulting in underestimation of the true activity (partial recovery). Second, a proportion of the activity originating from the adjacent regions will be recorded in the ROI (spill-in), resulting in an overestimation of the true activity (contamination). The net effect of partial recovery and contamination depends on the gradient of true activity between the ROI and the adjacent regions. The GTM describes the structure of the activity exchange between the regions, based on their spatial relations and the image resolution. Multiplying the measured activity by the inverse of the GTM provides an estimate of the true activity distribution (Rousset et al., 1998; Mawlawi et al., 2001).

On [^{11}C]raclopride images, the striatum as a whole is surrounded by background activity. Partial volume effects correction resulted in a significant increase in V_3'' but no change in $\Delta V_3''$. This result indicates that PVE correction is not required for experiments with a within-subject design in which the ROI is surrounded by background activity that is not affected by the challenge. We previously proposed that the estimate of 5-HT_{1A} receptor occupancy by pindolol in the dorsal raphe nuclei measured with [^{11}C]WAY 100635 is not biased by the very large PVE in this region, since this structure is located in the middle of a large region devoid of specific binding (Martinez et al., 2001). The observation that PVE correction did not change $\Delta V_3''$ in the striatum as a whole confirms this hypothesis. The situation, however, is more complex for the striatal subregions, since they are surrounded by other regions with specific binding.

Partial volume effects correction resulted in significant changes in $\Delta V_3''$ in 4 of 5 subregions. Partial volume effects correction had no impact on post-CA $\Delta V_3''$, a region that, similar to the striatum as a whole, is almost completely surrounded by background activity. In the other associative regions (pre-DCA and pre-DPU), PVE correction resulted in small but significant decreases in $\Delta V_3''$, due to the removal of contamination from the high-displacement regions (post-PU and the VST). Conversely, in the post-PU and the VST, PVE correction significantly increased $\Delta V_3''$, owing to the removal of contamination from the low-displacement regions (pre-DCA and pre-DPU). Thus, for adjacent regions differentially affected by a challenge, PVE correction enhances the detection of between-region differences in $\Delta V_3''$.

Mechanisms underlying between-region differences in $\Delta V_3''$

The technique used in this study does not directly measure dopamine release, but rather its impact on [^{11}C]raclopride binding. Therefore, the mechanisms potentially accounting for regional differences in $\Delta V_3''$ fall into two general categories: regional differences in the potency of dopamine to reduce [^{11}C]raclopride binding (postsynaptic factors) or regional differences in amphetamine-induced dopamine release (presynaptic factors). Data from this study do not allow us to differentiate between these scenarios, and the microdialysis literature is, in this regard, inconclusive. The fact that amphetamine may induce larger dopamine release in the nucleus accumbens compared with the caudate-putamen is supported by some (Sharp et al., 1987; Di Chiara and Imperato, 1988) but not all (Robinson and Camp, 1990)

rodent microdialysis studies (see discussion in Drevets et al., 2001). In primates, Bradberry et al. (2000) showed with microdialysis that systemic cocaine administration resulted in a greater increase in dopamine release in the ventral striatum compared to the dorsal striatum rostral to the AC, a finding consistent with this study. We are unaware of microdialysis studies comparing stimulant-induced dopamine release in the AST and SMST in primates. Such a study would be helpful to the interpretation of the results reported here.

Postsynaptic factors. Several postsynaptic factors may account for the differences in $\Delta V_3''$ between the VST and the AST. First, the relative contribution of D_3 receptors to the total D_2-like population is larger in the VST (32%) than in the caudate (18%) and the putamen (12%; Gurevich and Joyce, 1999). Because the affinity of dopamine for D_3 receptors is higher than for D_2 receptors (Sokoloff et al., 1990), the higher density of D_3 receptors in the VST may result in a higher potency of dopamine to displace [^{11}C]raclopride in this region. This factor, however, does not account for the higher $\Delta V_3''$ in the SMST compared with the AST. Second, baseline dopamine levels, measured with microdialysis, were reported to be lower in the VST compared with the AST (Bradberry et al., 2000). The law of mass action predicts that unoccupied D_2 receptors will display a higher affinity for dopamine in regions with lower baseline dopamine. Again, it is unclear if this factor accounts for the difference seen in the AST versus SMST. Other, more hypothetical factors, may involve regional differences in [^{11}C]raclopride binding vulnerability to changes in synaptic dopamine. For example, regional differences may exist in the proportion of D_2 receptors configured in high- and low-affinity states for dopamine, or in the proportion of synaptic and extrasynaptic D_2 receptors. Finally, other phenomena, such as receptor internalization (Laruelle, 2000) or polymerization (Logan et al., 2001) may be involved in the reduction in [^{11}C]raclopride binding after amphetamine, and these factors may be relevant to the between-region differences observed in this study.

Presynaptic factors. The regional differences in $\Delta V_3''$ observed in this study may reflect regional differences in dopamine release, that is, regional differences in the response of midbrain dopamine neurons to amphetamine exposure. Dopamine cells of the primate midbrain are divided into dorsal and ventral tiers (for review, see Haber et al., 2000). The dorsal tier includes the ventral tegmental area (VTA) and the dorsal substantia nigra pars compacta (SNc), whereas the ventral tier contains the densocellular zone of the SNc and the cell columns of the substantia nigra reticularis. The VST receives most of its input from the VTA and the dorsal SNc, the AST from the densocellular zone of the SNc, and the SMST from the densocellular zone of the SNc and the cell columns of the substantia nigra reticularis.

Dopamine neurons projecting to the VST (dorsal tier of the SN) express fewer D_2 autoreceptors and dopamine transporters (DAT) than the dopamine neurons of the nigrostriatal system (Hurd et al., 1994; Haber et al., 1995). Lower D_2 autoreceptor function is compatible with higher amphetamine-induced dopamine release because stimulation of these receptors decreases the firing activity of dopamine neurons (Bunney and Aghajanian, 1978). It is difficult to predict the effect of lower DAT expression on the amphetamine effect. Since amphetamine promotes dopamine efflux via reverse transport through the DAT (Sulzer et al., 1995), lower DAT density would be expected to be associated with lower amphetamine-induced dopamine release. In contrast, a higher density of DAT unoccupied by amphetamine may preserve more reuptake activity in regions with high DAT. In any case, these differences in D_2 autoreceptors and DAT expression between dopamine neurons of the dorsal and ventral tier do not fully explain the regional differences in $\Delta V_3''$ observed in this study.

An integrative hypothesis. The differences in the amphetamine effect between the VST, AST, and SMST may also result from the asymmetrical interactions between these regions and the midbrain (Haber et al., 2000). Each striatal subregion sends γ-aminobutyric acid (GABA)-ergic projections back to the VTA/SN (Fig. 8). The VST sends both reciprocal projections to the region from which it receives its dopamine input (VTA) and nonreciprocal projections to the regions where dopamine neurons projecting to the AST are located (densocellular zone). Thus, dopamine input to the AST is regulated by the VST. The AST projects back to the region from which it receives its dopamine input and to the region where dopamine projections to the SMST are located (cell columns of SNr). This suggests that dopamine input to the SMST is regulated by the AST. In contrast, the SMST projections to the midbrain are confined to the regions from which it receives its dopamine input. Through this feed-forward spiral of nonreciprocal connections, dopamine-mediated information progresses from the limbic to cognitive to sensorimotor areas of the striatum: the VST regulates the AST, and the AST regulates the SMST.

GABAergic neurons descending from the striatum to the VTA/SN make direct contact with dopamine neurons (a direct inhibitory effect on dopamine neurons), or make contact with GABAergic interneurons (an indirect inhibitory or stimulatory effects on dopamine activity). Given the inhibition of dopamine cell firing observed after amphetamine (Bunney and Aghajanian, 1978), it is likely that, under this condition, the inhibitory influence predominates. Whereas each dopamine cell group receives inhibitory feedback from the area it projects to via reciprocal connections, dopamine cells projecting to the AST may receive additional inhibition from the VST.

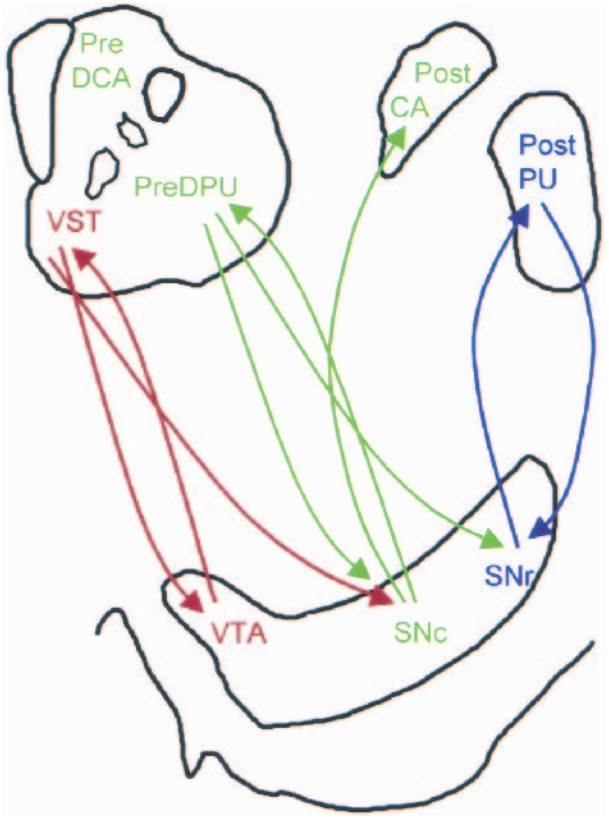

FIG. 8. Simplified representation of striatonigrostriatal subcircuits. The structures at the top represent the precommisural (left) and postcommissural (right) striata; the structure at the bottom represents the ventral tegmental area (VTA)–substantia nigra (SN). Limbic, associative (AST), and sensorimotor (SMST) subdivisions of the striatum are color-coded in red, green, and blue, respectively. Ascending arrows represent dopamine projections from the VTA/SN to the striatum and descending arrows represent γ-aminobutyric acid (GABA)-ergic projections from the striatum to the VTA/SN. Each striatal subdivision sends reciprocal GABAergic projections to the region of the midbrain from where they receive their dopamine inputs. In addition, the ventral striatum (VST) sends nonreciprocal connections to the midbrain region where dopamine neurons projecting the AST are located, and the AST sends nonreciprocal connections to the midbrain region where dopamine neurons projecting the SMST are located. Through this feed-forward spiral of nonreciprocal connections, dopamine-mediated information progresses from the limbic to cognitive to sensorimotor areas of the striatum. This organization provides a framework for a hypothetical interpretation of the amphetamine data reported in this study. It is proposed that, after amphetamine, each dopamine cell group receives inhibitory feedback from the area it projects to via reciprocal connections. In addition, the dopamine cell group projecting to the AST will receive inhibitory influence from the VST. This supplemental inhibitory influence may result in lower dopamine release in the AST, which, in turn, would weaken the inhibitory influence of the AST to dopamine cells projecting to the SMST. Thus, a pattern of asymmetrical inhibitions after amphetamine may result in an on-off-on phenomenon along the limbic–associative–motor cascade. Pre-DCA, precommissural dorsal caudate; pre-DPU, precommisural dorsal putamen; post-CA, postcommissural caudate; post-PU, postcommissural putamen; SNr, substantia nigra reticularis; SNc, substantia nigra pars compacta. (Adapted from Fig. 12 in Haber et al., 2000.)

This additional inhibition could result in lower dopamine release in the AST compared with the VST. Because of this relatively lower dopamine release in the AST, the inhibitory influence from the AST to the dopamine cells projecting to the SMST would be relatively weaker, resulting in higher dopamine release in the SMST compared with the AST. Such an asymmetrical regulation of midbrain dopamine neurons could result in the pattern of dopamine release seen in this study. Further research is necessary to test this hypothesis.

Relation with subjective experience

In this study, no associations were observed between baseline V_3'' values and the subjective effects of amphetamine. This result contrasts with the report of Volkow et al. (1999*a*), who observed that low baseline D_2 receptor availability was associated with a larger euphoric response after injection of methylphenidate.

In contrast, a significant association was observed between increased euphoria and higher $\Delta V_3''$ in the VST, SMST, and striatum as a whole. Plasma amphetamine levels did not account for this association. This result confirms and extends results of three previous imaging studies in healthy subjects. Using SPECT and [^{123}I]IBZM, Laruelle et al. (1995) reported a significant association between striatal $\Delta V_3''$ and the increase in euphoria induced by amphetamine. Using [^{11}C]raclopride, Volkow et al. (1999*b*) reported an association between increase in "high" ratings and striatal $\Delta V_3''$ induced by methylphenidate. Drevets et al. (2001) reported that the change in euphoria correlated with $\Delta V_3''$ of [^{11}C]raclopride in the VST and in the ventral putamen. Because the ventral putamen as defined in Drevets et al. (2001) overlaps significantly with the post-PU in this study, both studies concur that this association is stronger in post-PU and VST compared with the associative regions.

It is notable that four studies (Laruelle et al., 1995; Volkow et al., 1999b; Drevets et al., 2001, and the present study) observed a relation between $\Delta V_3''$ and the subjective euphoric experience in psychostimulant-naive subjects. Previous studies conducted in psychostimulant-naive subjects under controlled environmental conditions have identified large between-subject differences in the euphoric effects of amphetamine (Wachtel and de Wit, 1999). The results of these imaging studies show that this variability is at least partially accounted for by the magnitude of dopamine release and stimulation of D_2 receptor transmission elicited by amphetamine. To the extent that the rewarding effects of a drug is a predictor of subsequent use (Davidson et al., 1993), these data indicate that a strong neurobiologic response of the dopamine system to amphetamine may constitute a risk factor in the development of addiction.

CONCLUSIONS

This study revealed dynamic differences in dopamine transmission among functional subdivisions of the human striatum: amphetamine induced a larger displacement of [^{11}C]raclopride in the limbic and sensorimotor subdivisions than in the associative subdivision. We conclude that these regional differences in $\Delta V_3''$ are unlikely to result from an artifact of the imaging process. These differences were observed using both the paired-bolus–plus–infusion method (the present study) and the paired-single-bolus method (Drevets et al., 2001). In the present study, they were observed regardless of the method of analysis used to derive V_3'' (equilibrium or SRTM) and of the image analysis technique (ROI-based and voxel-based analyses). They did not result from a partial volume effect, since PVE correction magnified these differences.

Further research is warranted to establish the mechanisms involved in these regional differences and to explore their consequences in the development of the addiction. Striatal dopamine has been postulated to improve the signal-to-noise ratio of corticostriatal information flow and to promote synaptic plasticity of these pathways (Arbuthnott et al., 2000). Therefore, a differential effect of amphetamine among these functional subdivisions of the striatum may, on repeated exposure, fundamentally alter the normal limbic–associative–motor integration. The results of the present study also raise interesting questions relative to the increase in amphetamine-induced dopamine release measured in patients with schizophrenia in the striatum as a whole (Laruelle et al., 1996; Breier et al., 1997; Abi-Dargham et al., 1998). Because of the small contribution of the VST to the overall striatal signal, the dysregulation of dopamine release observed in these patients is unlikely to be restricted to mesolimbic projections. Given that the AST provides the larger contribution to the overall striatal volume, it is tempting to speculate that a disruption of dopamine release in this area is involved in schizophrenia. Finally, the observation of a relation between increase in euphoria experienced by the subjects and stimulation of D_2 receptors by dopamine in some, but not all, dopaminergic pathways illustrates the potential of PET dynamic neuroreceptor imaging as a tool to study the neurochemical circuits underlying human emotion.

Acknowledgments: The authors would like to thank Grace Abrena, David Amstel, Sue Chung, Nicole Eftychiou, Ingrid Gelbard-Stokes, Elizabeth Hackett, Leyla Khenissi, Kimchung Ngo, Julie Montoya, Chaka Peters, Audrey Perez, Beatriu Reig, Janine Rodenhiser-Hill, Norm Simpson, and Kris Wolff for excellent technical assistance.

REFERENCES

Abi-Dargham A, Gil R, Krystal J, Baldwin R, Seibyl J, Bowers M, van Dyck C, Charney D, Innis R, Laruelle M (1998) Increased striatal dopamine transmission in schizophrenia: confirmation in a second cohort. *Am J Psychiatry* 155:761–767

Anand A, Verhoeff P, Seneca N, Zoghbi SS, Seibyl JP, Charney DS, Innis RB (2000) Brain SPECT imaging of amphetamine-induced dopamine release in euthymic bipolar disorder patients. *Am J Psychiatry* 157:1108–1114

Arbuthnott GW, Ingham CA, Wickens JR (2000) Dopamine and synaptic plasticity in the neostriatum. *J Anat* 196(Pt 4):587–596

Bradberry CW, Barrett-Larimore RL, Jatlow P, Rubino SR (2000) Impact of self-administered cocaine and cocaine cues on extracellular dopamine in mesolimbic and sensorimotor striatum in rhesus monkeys. *J Neurosci* 20:3874–3883

Breier A, Su TP, Saunders R, Carson RE, Kolachana BS, de Bartolomeis A, Weinberger DR, Weisenfeld N, Malhotra AK, Eckelman WC, Pickar D (1997) Schizophrenia is associated with elevated amphetamine-induced synaptic dopamine concentrations: evidence from a novel positron emission tomography method. *Proc Natl Acad Sci U S A* 94:2569–2574

Bunney BS, Aghajanian GK (1978) *d*-Amphetamine-induced depression of central dopamine neurons: evidence for mediation by both autoreceptors and a striato-nigral feedback pathway. *Naunyn Schmiedebergs Arch Pharmacol* 304:255–261

Carson RE, Channing MA, Blasberg RG, Dunn BB, Cohen RM, Rice KC, Herscovitch P (1993) Comparison of bolus and infusion methods for receptor quantitation: application to [^{18}F]cyclofoxy and positron emission tomography. *J Cereb Blood Flow Metab* 13:24–42

Carson RE, Channing ME, Vuong BK, Watabe H, Herscovitch P, Eckelman WC (2001) Amphetamine-induced dopamine release: duration of action assessed with [^{11}C]raclopride in anesthetized monkeys. In: *Physiological imaging of the brain with PET* (Gjedde A, Hansen SB, Knudsen GM, et al., eds), San Diego, CA: Academic Press, pp 205–209

Davidson ES, Finch JF, Schenk S (1993) Variability in subjective responses to cocaine: initial experiences of college students. *Addict Behav* 18:445–453

Di Chiara G, Imperato A (1988) Drugs abused by humans preferentially increase synaptic dopamine concentrations in the mesolimbic system of freely moving rats. *Proc Natl Acad Sci U S A* 85:5274–5278

Drevets WC, Gautier C, Price JC, Kupfer DJ, Kinahan PE, Grace AA, Price JL, Mathis CA (2001) Amphetamine-induced dopamine release in human ventral striatum correlates with euphoria. *Biol Psychiatry* 49:81–96

Gurevich EV, Joyce JN (1999) Distribution of dopamine D_3 receptor expressing neurons in the human forebrain: comparison with D_2 receptor expressing neurons. *Neuropsychopharmacology* 20:60–80

Haber SN, Ryoo H, Cox C, Lu W (1995) Subsets of midbrain dopaminergic neurons in monkeys are distinguished by different levels of mRNA for the dopamine transporter: comparison with the mRNA for the D_2 receptor, tyrosine hydroxylase and calbindin immunoreactivity. *J Comp Neurol* 362:400–410

Haber SN, Fudge JL, McFarland NR (2000) Striatonigrostriatal pathways in primates form an ascending spiral from the shell to the dorsolateral striatum. *J Neurosci* 20:2369–2382

Hurd YL, Pristupa ZB, Herman MM, Niznik HB, Kleinman JE (1994) The dopamine transporter and dopamine D-$_2$ receptor messenger RNAs are differentially expressed in limbic- and motor-related subpopulations of human mesencephalic neurons. *Neuroscience* 63:357–362

Joel D, Weiner I (2000) The connections of the dopaminergic system with the striatum in rats and primates: an analysis with respect to the functional and compartmental organization of the striatum. *Neuroscience* 96:451–474

Kegeles LS, Zea-Ponce Y, Abi-Dargham A, Rodenhiser J, Wang T, Weiss R, Van Heertum RL, Mann JJ, Laruelle M (1999) Stability of [^{123}I]IBZM SPECT measurement of amphetamine-induced striatal dopamine release in humans. *Synapse* 31:302–308

Lammertsma AA, Hume SP (1996) Simplified reference tissue model for PET receptor studies. *Neuroimage* 4:153–158

Laruelle M (2000) Imaging synaptic neurotransmission with *in vivo* binding competition techniques: a critical review. *J Cereb Blood Flow Metab* 20:423–451

Laruelle M, Abi-Dargham A, Al-Tikriti MS, Baldwin RM, Zea-Ponce Y, Zoghbi SS, Charney DS, Hoffer PB, Innis RB (1994) SPECT quantification of [^{123}I]iomazenil binding to benzodiazepine receptors in nonhuman primates. Part II: equilibrium analysis of constant infusion experiments and correlation with *in vitro* parameters. *J Cereb Blood Flow Metab* 14:453–465

Laruelle M, Abi-Dargham A, van Dyck CH, Rosenblatt W, Zea-Ponce Y, Zoghbi SS, Baldwin RM, Charney DS, Hoffer PB, Kung HF, Innis RB (1995) SPECT imaging of striatal dopamine release after amphetamine challenge. *J Nucl Med* 36:1182–1190

Laruelle M, Abi-Dargham A, van Dyck CH, Gil R, De Souza CD, Erdos J, Mc Cance E, Rosenblatt W, Fingado C, Zoghbi SS, Baldwin RM, Seibyl JP, Krystal JH, Charney DS, Innis RB (1996) Single photon emission computerized tomography imaging of amphetamine-induced dopamine release in drug-free schizophrenic subjects. *Proc Natl Acad Sci U S A* 93:9235–9240

Laruelle M, Iyer RN, Al-Tikriti MS, Zea-Ponce Y, Malison R, Zoghbi SS, Baldwin RM, Kung HF, Charney DS, Hoffer PB, Innis RB, Bradberry CW (1997) Microdialysis and SPECT measurements of amphetamine-induced dopamine release in nonhuman primates. *Synapse* 25:1–14

Logan J, Fowler JS, Dewey SL, Volkow ND, Gatley SJ (2001) A consideration of the dopamine D_2 receptor monomer-dimer equilibrium and the anomalous binding properties of the dopamine D_2 receptor ligand, *N*-methyl spiperone. *J Neural Transm* 108:279–286

Martinez D, Hwang D, Mawlawi O, Slifstein M, Kent J, Simpson N, Parsey RV, Hashimoto T, Huang Y, Shinn A, Van Heertum R, Abi-Dargham A, Caltabiano S, Malizia A, Cowley H, Mann JJ, Laruelle M (2001) Differential occupancy of somatodendritic and postsynaptic 5HT($_{1A}$) receptors by pindolol: a dose-occupancy study with [^{11}C]WAY 100635 and positron emission tomography in humans. *Neuropsychopharmacology* 24:209–229

Mawlawi O, Martinez D, Slifstein M, Broft A, Chatterjee R, Hwang DR, Huang Y, Simpson N, Ngo K, Van Heertum R, Laruelle M (2001) Imaging human mesolimbic dopamine transmission with positron emission tomography. Part I: accuracy and precision of D(2) receptor parameter measurements in ventral striatum. *J Cereb Blood Flow Metab* 21:1034–1057

Parsey RV, Oquendo MA, Zea-Ponce Y, Rodenhiser J, Kegeles LS, Pratap M, Cooper TB, Van Heertum R, Mann JJ, Laruelle M (2001) Dopamine D(2) receptor availability and amphetamine-induced dopamine release in unipolar depression. *Biol Psychiatry* 50:313–322

Robinson TE, Camp DM (1990) Does amphetamine preferentially increase the extracellular concentration of dopamine in the mesolimbic system of freely moving rats? *Neuropsychopharmacology* 3:163–173

Rousset OG, Ma Y, Evans AC (1998) Correction for partial volume effects in PET: principle and validation. *J Nucl Med* 39:904–911

Sharp T, Zetterstrom T, Ljungberg T, Ungerstedt U (1987) A direct comparison of amphetamine-induced behaviours and regional brain dopamine release in the rat using intracerebral dialysis. *Brain Res* 401:322–330

Singer HS, Szymanski S, Giuliano J, Yokoi F, Dogan AS, Brasic JR, Zhou Y, Grace AA, Wong DF (2002) Elevated intrasynaptic dopamine release in Tourette's syndrome measured by PET. *Am J Psychiatry* 159:1329–1336

Sokoloff P, Giros B, Martres M-P, Bouthenet M-L, Schwartz J-C (1990) Molecular cloning and characterization of a novel dopamine receptor D_3 as a target for neuroleptics. *Nature* 347:146–151

Sulzer D, Chen TK, Lau YY, Kristensen H, Rayport S, Ewing A (1995) Amphetamine redistributes dopamine from synaptic vesicles to the cytosol and promotes reverse transport. *J Neurosci* 15:4102–4108

Volkow ND, Wang G-J, Fowler JS, Logan J, Schlyer D, Hitzemann R, Lieberman J, Angrist B, Pappas N, MacGregor R, Burr G, Cooper T, Wolf AP (1994) Imaging endogenous dopamine competition with [^{11}C]raclopride in the human brain. *Synapse* 16:255–262

Volkow ND, Wang GJ, Fowler JS, Logan J, Gatley SJ, Hitzemann R, Chen AD, Dewey SL, Pappas N (1997) Decreased striatal dopaminergic responsiveness in detoxified cocaine-dependent subjects. *Nature* 386:830–833

Volkow ND, Wang GJ, Fowler JS, Logan J, Gatley SJ, Gifford A, Hitzemann R, Ding YS, Pappas N (1999*a*) Prediction of reinforcing responses to psychostimulants in humans by brain dopamine D_2 receptor levels. *Am J Psychiatry* 156:1440–1443

Volkow ND, Wang GJ, Fowler JS, Logan J, Gatley SJ, Wong C, Hitzemann R, Pappas NR (1999*b*) Reinforcing effects of psychostimulants in humans are associated with increases in brain dopamine and occupancy of D(2) receptors. *J Pharmacol Exp Ther* 291:409–415

Wachtel SR, de Wit H (1999) Subjective and behavioral effects of repeated *d*-amphetamine in humans. *Behav Pharmacol* 10:271–281

Watabe H, Endres CJ, Breier A, Schmall B, Eckelman WC, Carson RE (2000) Measurement of dopamine release with continuous infusion of [^{11}C]raclopride: optimization and signal-to-noise considerations. *J Nucl Med* 41:522–530

Woods RP, Cherry SR, Mazziotta JC (1992) Rapid automated algorithm for aligning and reslicing PET images. *J Comput Assist Tomogr* 16:620–633

Woods RP, Mazziotta JC, Cherry SR (1993) MRI-PET registration with automated algorithm. *J Comput Assist Tomogr* 17:536–546